The 2017 World Congress on
Advances in Structural Engineering and Mechanics (ASEM17)
28 August - 1 September, 2017, Ilsan(Seoul), Korea

Micromechanical modeling of reinforced silk with partially aligned carbon nanotubes

*Sangryun Lee[1)] and Seunghwa Ryu[2)]

[1), 2)] *Department of Mechanical Engineering, KAIST, Daejeon 34141, Korea*
[2)] *ryush@kaist.ac.kr*

ABSTRACT

Recently, reinforced silk with graphene or carbon nanotubes (CNT) has gained significant attention as a new type of composites combining natural and man-made super materials. We estimate the effective mechanical properties of silk-graphene or silk-CNT composites with micromechanical approach based on Mori-Tanaka method. First, we consider uniform distribution of CNT reinforcements and perfectly bonded interfaces between silk matrix and reinforcement to estimate the ideal effective properties. We compute the Young's modulus and the ideal strength of the composite as a function of volume fractions and orientation distribution of reinforcements. The effective stress-strain curve of the composite is determined using 2nd order stress moment obtained from the field fluctuation method. The fracture properties of the composite is calculated by comparing the effective stress of the silk in the composite with its strength in pure phase. Second, to account for the realistic composites in experiments, we consider the effect of damaged interface between matrix and reinforcement and agglomeration of reinforcements. Non-perfect bonding is considered in the framework of the modified Mori-Tanaka approach taking linear spring interface model. Our study suggests the upper bound of mechanical properties of reinforced silk, and possible explanations on the highly variable stiffness and modulus of reinforced silk observed in experiments.

1. INTRODUCTION

Recently, reinforced silk with graphene or carbon nanotube(CNT) has gained significant attention as a new type of composites combining natural and man-made super materials. (E. Lepore 2015) Some of research found that the effective mechanical properties of the composite have been significantly improved against those of pure matrix, spider silk. For efficient design of the composite, it is necessary to understanding the theoretical background of the improved properties.
To compute the effective properties theoretically, various micromechanics-based

---

[1)] Graduate Student
[2)] Professor

homogenization approaches have been used, such as the Self-Consistent (SC) method, the Mori-Tanaka (MT) method, and the Eshelby method. The MT method is the most popular method because it provides more accurate predictions on the effective stiffness than the Eshelby method and has an explicit and closed-form expression, whereas the SC method relies on implicit equations. However, the original MT method has two limitations: first, it does not account for the imperfections in the filler-matrix interface, such as debonding and slip; second, it is only applicable when all fillers in the matrix are aligned perfectly along one direction.

In this work, we propose an improved micromechanics model to correct the two problems regarding the interfacial damage and the orientation average. We demonstrate that the singularities in effective modulus prediction can be removed when the corrected R tensor is used. We obtain the analytic expressions of R tensor for axisymmetric ellipsoidal fillers and validate our results against the numerical integration results. We also confirm that our expressions satisfy two limiting cases, i.e., aspect ratio of 1 and infinity, at which analytic forms are readily available. (Qu 1993) Instead of the $3-1-3$ Euler angle in previous research, we use polar and azimuthal angles on the unit sphere to represent the inclusion orientation and derive algebraic expressions for the general transversely isotropic 4th order tensor under axisymmetric filler orientation distribution. We confirm that the longitudinal and transverse elastic moduli from our model converge in the random orientation distribution limit. Our results can be widely used to describe composites that include particles and fillers at various aspect ratios.

Beyond the linear elastic limit, we calculate effective nonlinear properties such as toughness, strength, and elongation for the composite having interfacial damage. The method used for this calculations are secant modulus method and field fluctuation method which are popular in micromechanics society. By implementing these into homogenization method, we calculate effective stress strain curve of the composite for various orientation distributions of fillers. Unlike previous researches which predict effective stress strain curve for isotropic composite, here we firstly calculate the curve of anisotropic composite considering external loading direction, axial direction or transverse direction. To predict the toughness and strength of the composite, we study failure behavior of the composite by determining failure of each phase for different interfacial damage value. We find that the toughness of the composite significantly increases at the finite interfacial damage whereas the composite has maximum strength at perfect bonding case.

2. PROPOSED FAILURE SURFACE

The equation for Mori-Tanaka method is expressed as (1),

$$L_{eff} = (c_0 L_0 + c_1 L_1 : A) : (c_0 I + c_1 A)^{-1} \quad (1)$$

where L_0 and L_1 are matrix and inclusion stiffness tensor and I is the symmetric identity tensor. c_0 and c_1 refer to the volume fraction of matrix and inclusions, respectively; thus, $c_0 + c_1 = 1$. A is the strain concentration tensor which relates the external strain (ε^{ext}) applied to the composite and the volume-averaged strain (ε_1) within the inclusions by the definition of $\varepsilon_1 \equiv A : \varepsilon^{ext}$. After solving linear elasticity for single inclusion problem, the A tensor can be expressed in terms of Eshelby tensor (S) and stiffness tensor of matrix(L_0) and inclusion(L_1), as Eq.(2).

$$A = [I + S{:}\, L_0^{-1}{:}\, (L_1 - L_0)]^{-1} \tag{2}$$

The Eshelby tensor (S) for the axisymmetric ellipsoidal filler has been derived in the literature (Qiu 1990)

Because the original MT method is only applicable when all the fillers are completely aligned and have perfect bonding with the matrix, the modified Mori-Tanaka (mMT) approach must be employed to account for the interfacial damage at the interface (slip or debonding). To model such interfacial damage, we consider the displacement jump across the interface by adopting the linear spring model (Qu 1993) (see Fig.1),

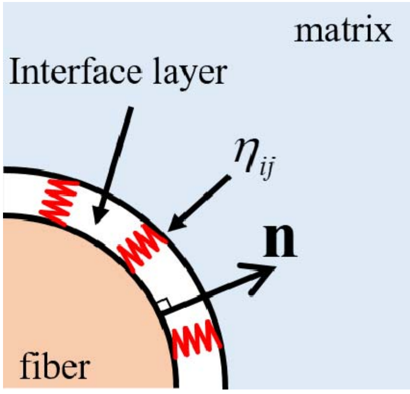

Fig. 1 Schematic of interface spring model

$$\Delta u_i = \eta_{ij}\sigma_{jk}n_k,\ \ \eta_{ij} = \alpha\delta_{ij} + (\beta - \alpha)n_i n_j \tag{3}$$

where the η_{ij} refers to the compliance of the interface spring composed of the tangential (α) and normal (β) directions. The n_i represents outward direction unit normal vector at the inclusion surface. After solving eigenstrain problem with the interfacial springs, the modified Eshelby tensor ($\tilde{S}$) is given as follows,

$$\tilde{S} = S + (I - S){:}\, R{:}\, L_0{:}\, (I - S). \tag{4}$$

Here R tensor represents intensity of interfacial damage and a function of the inclusion shape and the compliance of interfacial springs. The tensor is expressed as Eq(5) if there is only tangential linear spring and in this work, we reformulate the R tensor for the case of ellipsoidal inclusion to correct the results from previous studies.

$$R_{ijkl} = \alpha(P_{ijkl} - Q_{ijkl}) \tag{5}$$

where

$$P_{ijkl} = \frac{3}{16\pi}\int_0^{\pi}\left[\int_0^{2\pi}\left(\delta_{ik}\widehat{n_j}\widehat{n_k} + \delta_{jk}\widehat{n_i}\widehat{n_l} + \delta_{il}\widehat{n_k}\widehat{n_j} + \delta_{jl}\widehat{n_k}\widehat{n_i}\right)n^{-1}d\theta\right]sin\phi d\phi \tag{6}$$

and

$$Q_{ijkl} = \frac{3}{4\pi}\int_0^{\pi}\left[\int_0^{2\pi}\widehat{n_i}\widehat{n_j}\widehat{n_k}\widehat{n_l}n^{-3}d\theta\right]sin\phi d\phi. \tag{7}$$

with $\hat{\boldsymbol{n}} = \left(\frac{cos\phi}{a_1}, \frac{sin\phi cos\theta}{a}, \frac{sin\phi sin\theta}{a}\right)^T, n = \sqrt{\widehat{n_i}\widehat{n_i}} = \frac{1}{\rho a}\sqrt{\cos^2\phi + \rho^2\sin^2\phi}$, and $\rho = \frac{a_1}{a}$.

The non-zero independent components of P and Q can be obtained from the integral given below:

$$P_{1111} = \frac{3}{2a}\frac{1}{\rho^2-1}\left[\frac{\rho^2}{\sqrt{\rho^2-1}} sin^{-1}\frac{\sqrt{\rho^2-1}}{\rho} - \frac{1}{\rho}\right],\ P_{2222} = \frac{3}{2a}\left[\frac{\rho}{\sqrt{\rho^2-1}}\frac{\rho^2-2}{2(\rho^2-1)} sin^{-1}\frac{\sqrt{\rho^2-1}}{\rho} + \frac{\rho}{2(\rho^2-1)}\right]$$

$$P_{1212} = \frac{1}{4}(P_{1111} + P_{2222}), P_{2323} = \frac{1}{2}P_{2222} \qquad (10)$$

$$Q_{1111} = \frac{3}{2a}\left[\frac{2\rho^2+1}{\rho(\rho^2-1)^2} - \frac{3\rho}{(\rho^2-1)^{5/2}} sin^{-1}\frac{\sqrt{\rho^2-1}}{\rho}\right],\ Q_{1122} = \frac{3}{4a}\left[\frac{\rho(\rho^2+2)}{(\rho^2-1)^{5/2}} sin^{-1}\frac{\sqrt{\rho^2-1}}{\rho} + \frac{-3\rho}{(\rho^2-1)^2}\right]$$

$$Q_{2222} = \frac{9}{8a}\left[\rho - \frac{\rho^3(2\rho^2-5)}{2(\rho^2-1)^2} + \frac{\rho^3(\rho^2-4)}{2(\rho^2-1)^{5/2}} sin^{-1}\frac{\sqrt{\rho^2-1}}{\rho}\right],\ Q_{2233} = \frac{1}{3}Q_{2222}.$$

Other components can be obtained by using the symmetry condition in the 2-3 plane as well as the minor and major symmetry of P and Q tensors. In the limit of zero spring compliance (i.e. $\alpha = 0$), the modified Eshelby tensor $(\tilde{S})$ becomes the original Eshelby tensor (S) because R becomes zero tensor. The effective moduli in the mMT scheme can be obtained by replacing the original Eshelby tensor (S) with the modified Eshelby tensor $(\tilde{S})$ (Qu 1993),

$$L_{eff} = \left(c_0L_0 + c_1L_1{:}\tilde{A}\right){:}\left(c_0I + c_1\tilde{A} + c_1R{:}L_1{:}\tilde{A}\right)^{-1} \qquad (9)$$

where $\tilde{A}$ is the modified strain concentration tensor, $\tilde{A} = \left[I + \tilde{S}{:}L_0^{-1}{:}(L_1 - L_0)\right]^{-1}$.

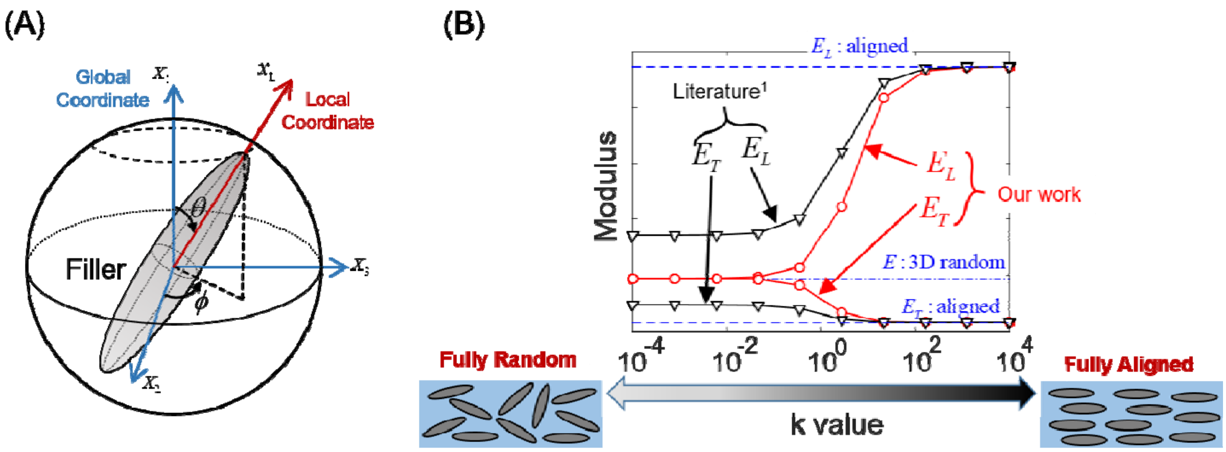

Fig. 2 (A) Coordinate system for orientation average scheme. (B) Effective modulus as a function of degree of alignment (k).

The modified Mori-Tanaka method is only applicable for the composites with completely aligned inclusions. However, in the realistic composites, fillers are partially aligned as depicted in Fig. 2. Because the inclusions in the liquid-state matrix are drawn along one axis (X_1) in most manufacturing processes and experiments, we limit our focus on the axisymmetric orientation distribution. Following the previous studies (Odegard 2003), we define the orientation averaged Mori-Tanaka (oaMT) as Eq. (10).

$$L_{eff} = \left(c_0L_0 + c_1 < L_1{:}\tilde{A} >\right){:}\left(c_0I + c_1 < \tilde{A} > + c_1 < R{:}L_1{:}\tilde{A} >\right)^{-1} \qquad (10)$$

where the operator $<>$ denotes the orientation average scheme of tensor. When the orientation distribution $\lambda(\theta)$ is function of θ only, i.e. for axis-symmetry distribution, the orientation average of an arbitrary 4th order tensor X can be defined as

$$< X >_{ijkl} = \frac{\int_0^{\frac{\pi}{2}} \int_{-\pi}^{\pi} X'_{ijkl}(\phi,\theta)\lambda(\theta)\sin(\theta)d\phi d\theta}{\int_0^{\frac{\pi}{2}} \int_{-\pi}^{\pi} \lambda(\theta)\sin\theta d\phi d\theta} \quad (11)$$

where θ and ϕ are azimuthal and polar angle with respect to the global coordinate (see Fig. 2(A)). X' is the tensor transformed to global coordinate system. Following the coordinate transformation rule of 4th order tensor with rotation matrix $\boldsymbol{c}$, X'_{ijkl} can be expressed as Eq.(12).

$$X'_{ijkl} = c_{ip}c_{jq}c_{kr}c_{ls}X_{pqrs} \quad \boldsymbol{c} = \begin{bmatrix} \cos\theta & -\sin\theta & 0 \\ \sin\theta\cos\phi & \cos\theta\cos\phi & -\sin\phi \\ \sin\theta\sin\phi & \cos\theta\sin\phi & \cos\phi \end{bmatrix} \quad (12)$$

The axisymmetric orientation distribution function can be categorized into three types: 3D random, normal distribution, and aligned.

$$\begin{aligned} &\lambda(\theta) = 1 \ \text{: 3D random distribution} \\ &\lambda(\theta) = \exp(-k\theta^2) \ \text{: normal distribution} \\ &\lambda(\theta) = \delta(\theta) \ \text{: aligned distribution} \end{aligned} \quad (13)$$

As visualized in Fig. 2(B), when k in the normal distribution function goes to zero or infinite, the distribution converges to random or fully aligned distributions, respectively. We note that previously used $3-1-3$ Euler angle set cannot describe the axisymmetric distribution along the X_1 axis due to the geometrical constraint, while several studies have adopted the $3-1-3$ Euler angle set to describe the composites with axisymmetric filler orientation distribution. When k goes to zero, i.e., for a random orientation distribution, the composite must behave as an isotropic material. However, the longitudinal and transverse Young's modulus from the previous study do not converge to the same value in the random orientation limit. In contrast, the oaMT with our orientation average scheme predicts that both longitudinal and transverse moduli approach the same modulus of the composite with randomly oriented fillers, whose analytic expression is available.

Table. 1 Material properties of spider silk and CNT.

Material properties	Spider silk	Carbon nanotube (CNT)
Young's modulus (E)	0.5 GPa	
Poisson's ratio (ν)	0.4	
Longitudinal Young's modulus (E_L)		1.06 TPa
Transverse bulk modulus (κ_{23})		271 GPa
Transverse shear modulus (μ_{23})		17 GPa
In plane shear modulus (μ_{12})		442 GPa
In plane Poisson's ratio (ν_{12})		0.162

We calculate effective moduli of reinforced silk having partially aligned CNT and interfacial damage by changing variables such as volume fraction, degree of alignment, and aspect ratio of CNT. (Table. 1) As shown in Fig. 3, the effective moduli of the composite which has interfacial damage predicted for the range of aspect ratio. The moduli for interfacial damage increase as the aspect ratio of inclusion increases and are lower than those of perfect bonding case. Unlike results from the mMT using previous R tensor model, the predicted moduli from our model are continuous for entire range of the aspect ratio and satisfies limiting case at aspect ratio of one.

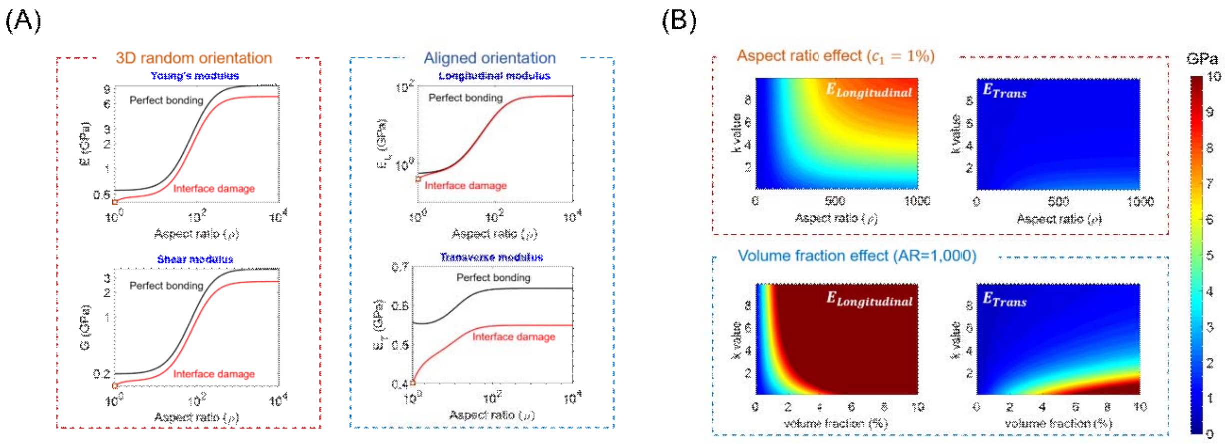

Fig. 3 (A) Elastic modulus for two limit orientation case as a function of aspect ratio fillers. (B) Two elastic modulus respect to aspect ratio, volume fraction, and degree of alignment.

To calculate effective stress strain curve of composite, we combine two methods, secant modulus method and field fluctuation method. Using secant modulus and field fluctuation method, we can construct homogenized material for every loading increment and predict volume-averaged stress within matrix and inclusions. This is the first time to predict the stress strain curves of anisotropic composites for different loading directions. We predict the effective stress-strain curves of reinforced silk with perfect adhesion conditions at the interface. Therefore, the predicted result will represent the upper bound solution. Calculations have been performed for various orientation distribution function by changing k value in normal distribution function. When axial loads applied to composites with partially aligned inclusions, the mechanical behavior becomes stiffer as more CNTs aligned with the axial axis, while transverse direction loads, the composite is softer. When the k value goes to zero, the difference between two curves (axial loading, lateral loading) diminishes and finally become same at random distribution(k=0).

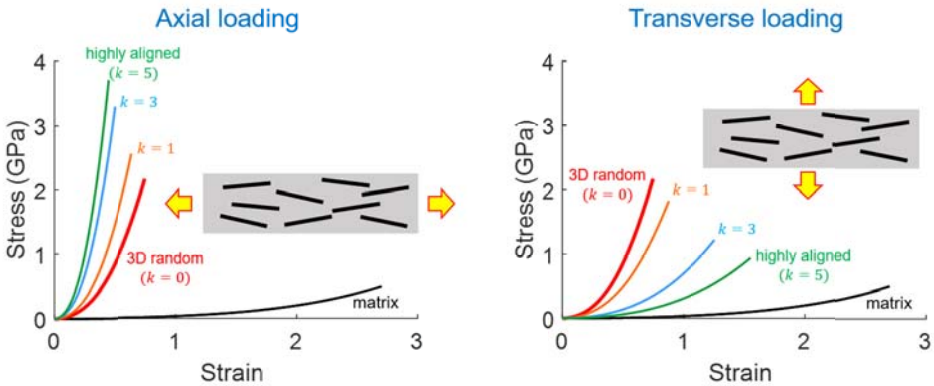

Fig. 4 Effective stress strain curve for different loading direction.

To investigate mechanical behavior of composite having interfacial damage, we consider the composite with fully aligned CNTs. As interfacial damage increases, the strength of the composite decreases. However, the toughness has maximum value at finite interfacial damage (see Fig. 5). To explain the reason, we calculate effective stress strain curve of reinforced silk for two different interfacial damage parameter. As shown Fig. 5, the composite show saw-tooth shape stress strain curve for moderate interfacial damage because the CNT breaks before matrix fails. After CNTs fail, we increase external loading until matrix fail with the assumption that the CNT with length of L are separated as two CNTs with each length of $L/2$. As a results, the toughness, which means energy absorption until failure show maximum at finite interfacial damage.

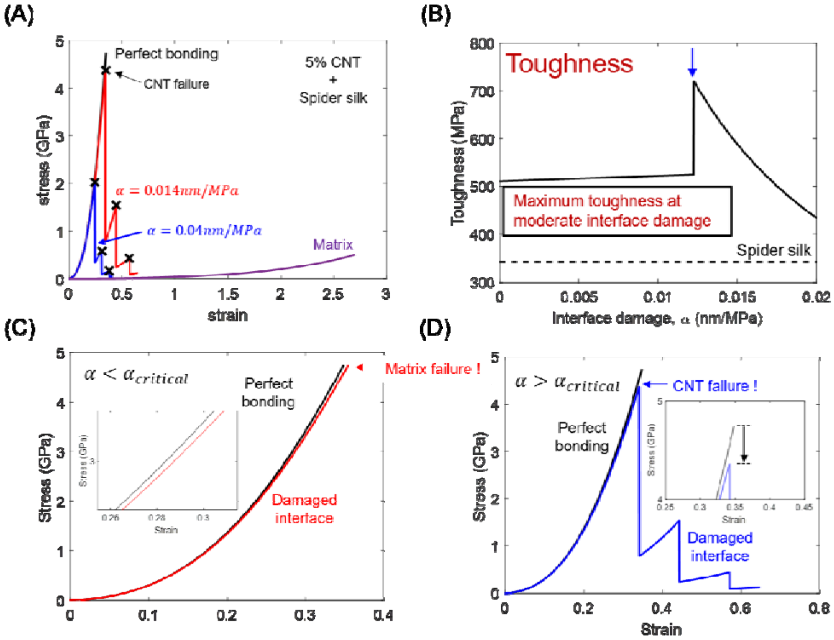

Fig. 5 (A) Effective stress strain curve for various interfacial damage. (B) Toughness as a function of interfacial damage. Stress-strain curve of composite having small(C) and large(D) interfacial damage.

3. CONCLUSIONS

We use micromechanics-based approaches to predict the effective properties of reinforced silk with CNT. We have solved the mathematical problems in the linear spring model for displacement jump at the interface and calculated the effective properties of the composite with partially aligned CNTs considering the orientation distribution. Beyond the linear elastic limit, we calculate the effective stress strain curve of a composite for various orientation distribution. By determining the failure of each phase and taking into account interface damage, we can describe the mechanism for toughening of the composite against pure silk.

REFERENCES

Emiliano, L., Francesco, B., Matteo, B., Federico, B., Simone, T., Giovanni, G., Andrea, C.F., Nicola, M.P. (2015), “Silk reinforced with graphene or carbon nanotubes spun by spiders”, *arXiv*:1504.06751.

Qu, J. (1993), “The effect of slightly weakened interfaces on the overall elastic properties of composite materials”, *Mechanics of Materials,* 14, 269-281.

Qiu, Y.P., Weng, G.J., (1990), “On the application of Mori-Tanaka's theory involving transversely isotropic spheroidal inclusions”, *International Journal of Engineering Science,* 28, 1121-1137.

Odegard, G.M., Gates, T.S., Wise, K.E., Park, C., Siochi, E.J., (2003), “Constitutive modeling of nanotube–reinforced polymer composites”, *Composites Science and Technology,* 63, 1671-1687.